Transport barrier using a vorticity source in 5D gyrokinetic simulations

G. Lo-Cascio[1], E. Gravier[1], T. Réveillé[1], M. Lesur[1], X. Garbet[2],
Y. Sarazin[2], K. Lim[3], L. Vermare[4], A. Guillevic[1], V. Grandgirard[2]

[1] *IJL, UMR 7198 CNRS, Université de Lorraine, 54000 Nancy, France*

[2] *CEA, IRFM, F-13108 Saint-Paul-lez-Durance, France*

[3] *Swiss Plasma Center, CH-1015 Lausanne, Switzerland*

[4] *Ecole Polytechnique, LPP, CNRS UMR 7648, 91128 Palaiseau, France*

Turbulent transport [1] is an important limiting factor for fusion reactor devices efficiency. It can be reduced through the presence of a transport barrier either in the core (ITB, Internal Transport Barrier) or at the edge (ETB, Edge Transport Barrier, H-mode [2]) characterized by a radially sheared electric field and a steep pressure gradient. As a consequence, a strong $E \times B$ sheared poloidal flow is generated. Different theoretical hypothesis have been proposed to explain the effects of shear flow on turbulent plasma. The focus here is on large scale turbulent structure suppression through $E \times B$ poloidal shearing [3]. GYSELA [4], a 5D full-f gyrokinetic code, is used in a flux-driven regime to inject such sheared flow and create a transport barrier in presence of ITG turbulence [5]. A vorticity source [6] is used to achieve such poloidal shearing.

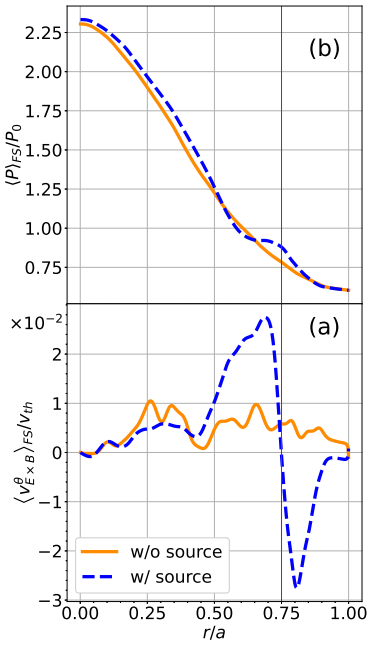

Figure 1: *Poloidal $E \times B$ drift velocity* ***(a)*** *and ion pressure* ***(b)*** *radial profiles* ***with source*** *(dashed blue line) and* ***without*** *(solid orange line) at $t\omega_{c,0} = 377920$. The vorticity source position is represented by the red vertical line.*

Model

GYSELA couples both the Vlasov and the quasi-electroneutrality equation. An adiabatic electron response is taken so that the time-averaged particle transport across circular magnetic surfaces vanishes up to compressional effects. Both equations are solved for the main ion species (i.e. Deuterium in our case):

$$B^{\star}_{\parallel}\partial_t \bar{F} + \nabla \cdot \left(\dot{\mathbf{x}}_{GC} B^{\star}_{\parallel} \bar{F}\right) + \partial_{v_{G\parallel}} \left(\dot{v}_{G\parallel} B^{\star}_{\parallel} \bar{F}\right) = \mathscr{C}\left(\bar{F}\right) + \mathscr{S}, \tag{1}$$

$$en_{e_0}\left(\frac{\phi - \langle\phi\rangle_{FS}}{T_e}\right) - Z_i \nabla_{\perp} \cdot \left(\frac{n_0}{B_0 \omega_{c,i}} \nabla_{\perp} \phi\right) = Z_i \int dv \, \mathscr{J}\left[\bar{F} - \bar{F}_{eq}\right], \tag{2}$$

With $\bar{F}$ the ion gyro-center distribution function, ϕ the electrostatic potential, $\mathbf{x}_{GC}$ and $v_{G\parallel}$ the gyro-center position and parallel velocity respectively. $\mathscr{J}$ and $\mathscr{C}\left(\bar{F}\right)$ are respectively the gyro-average and the collision operators, the latter conserving both energy and particles. $\mathscr{S}$

represents the source terms (i.e. heat and/or poloidal momentum / vorticity source). The average over a flux-surface is defined by $\langle \ldots \rangle_{FS} = \iint \ldots J_\chi d\theta d\varphi / \iint J_\chi d\theta d\varphi$ with $J_\chi = (\mathbf{B}\cdot\nabla\theta)^{-1}$ the flux-surface jacobian.

Vorticity source

The kinetic source term of poloidal momentum (i.e. vorticity) is defined as

$$\mathscr{S}_\Omega = \frac{m v_{G\|}^2 - \mu B}{T_s} S_r(r)\, S_0^\Omega \exp\left(-\frac{\frac{1}{2} m v_{G\|}^2 + \mu B}{T_s}\right) \tag{3}$$

with $\mu = m_i v_\perp^2 / 2B$ the magnetic moment, S_0^Ω the source amplitude, $S_r(r)$ the radial profile and T_s the source temperature. No heat nor particles are injected in the system with this source. The fluid vorticity conservation equation is given by

$$\partial_t W + \partial_r \mathscr{K} = S_0 \nabla_\perp^2 S_r \tag{4}$$

with $\mathscr{K} = e\left\langle \int dv^\star \mathscr{J}\left[(d_t \mathbf{x}_G \cdot \nabla r)\bar{F}\right]\right\rangle_{FS}$ the fluid vorticity flux, $W = e\left\langle \int dv \mathscr{J}\left[\bar{F}\right]\right\rangle_{FS}$ the fluid vorticity, and $S_0\nabla_\perp^2 S_r$ the fluid vorticity source term. To get equation (4), a gyro average of the Vlasov equation (1) is performed before integrating over the velocity space. To obtain a 1D (i.e. radial) equation for vorticity, a flux-surface average is also performed.

Transport barrier

When sheared poloidal fluxes are in place (figure 1a), a "plateau" appears on the radial ion pressure profile (figure 1b) at the source location and the core pressure slightly increases compared to the reference case (no source). Since the source does not inject energy in the system, the increase seen on the radial pressure profile should result from the presence of some transport barrier.

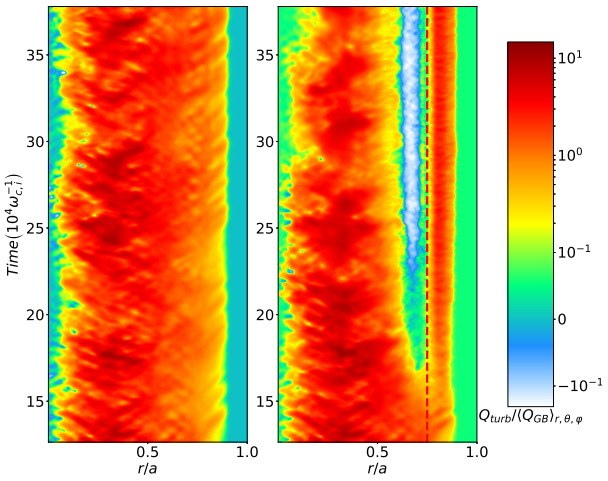

Figure 2: *Total radial heat flux Q_{tot} (equation 5) as a function of radius and time* ***with source*** *(right) and* ***without source*** *(left). The vorticity source radial position is indicated by the red vertical line.*

Turbulence quench

We compute the radial flux of energy with

$$Q^{tot} = \left\langle \int \mathscr{E}\left(v_D^r + v_E^r\right)\bar{F}_s dv \right\rangle_{FS} \tag{5}$$

where $\mathscr{E} = \mu B + \frac{1}{2} v_{G\|}^2$, $v_D^r = \bar{\mathbf{v}}_D \cdot \nabla r$ and $v_E^r = \bar{\mathbf{v}}_{E\times B} \cdot \nabla r$ which are respectively the curvature plus B gradient and $E \times B$ drift velocities projected alond the radial axis.

Figure 2 represents the total radial heat flux (equation 5) as a function of radius and time normalized to the average gyro-Bohm heat flux $\langle Q_{GB}\rangle_{r,\theta,\varphi} = \langle -n_{e,0}\chi_{GB}\nabla T_{e,0}\rangle_{r,\theta,\varphi}$ with $\chi_{GB} = \rho^{\star}\chi_B = \rho^{\star}\frac{T_{e,0}}{q_i B}$, the gyro-Bohm diffusivity. When the vorticity source is activated (figure 2b), the total heat flux is reduced by one order of magnitude compared to the reference (figure 2a) case in the source region. The total heat flux is also lower in the core region ($r/a = [0.25, 0.45]$) with the source activated than without.

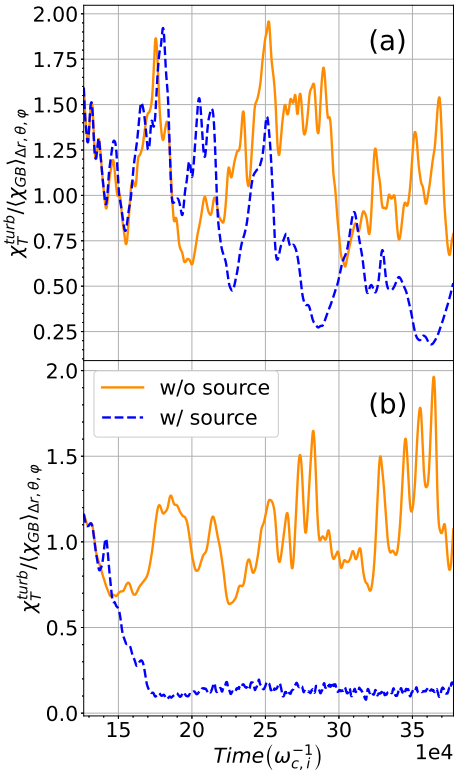

Figure 3: *Time evolution of the turbulent heat diffusivity in the* $r/a = [0.15, 0.6]$ ***(a)*** *and* $r/a = [0.7, 0.8]$ ***(b)*** *regions* ***with source*** *(blue dashed line) and* ***without*** *(solid orange line).*

Assuming diffusive heat fluxes, one can define the turbulent heat diffusivity component:

$$\chi_T^{turb} = -\left\langle Q^{turb}\right\rangle_{\Delta r} / \langle n\nabla T\rangle_{\Delta r} \tag{6}$$

with $Q^{turb} = \left\langle \int \mathscr{E}\left(v^r_{E_{n\neq 0}}\right)\bar{F}_s dv\right\rangle_{FS}$ where $v^r_{E_{n\neq 0}} = v^r_E - \langle v^r_E\rangle_{\varphi}$. The symbol $\langle\ldots\rangle_{\Delta r}$ represents an average over a radial interval. The heat diffusivity coefficients are normalized to the local $\langle\chi_{GB}\rangle_{\Delta r,\theta,\varphi}$ gyro-Bohm diffusivity coefficients.

In the source region, the turbulent diffusivity component (figure 3b) rapidly decreases by an order of magnitude in presence of sheared poloidal flows (i.e. with the source activated). The core turbulent diffusivity (figure 3a) also undergoes a much more softer decay. Those diffusivity drops explain the observed plateau at the source radial location and the slight core pressure increase as less energy is lost to the edge.

Structure changes

The perturbed electrostatic potential is defined through

$$\delta\phi\,(r,\theta,t) = \phi\,(r,\theta,\varphi=0,t) - \langle\phi\,(r,\theta,\varphi,t)\rangle_{\varphi} \tag{7}$$

where $\langle\phi\,(r,\theta,\varphi)\rangle_{\varphi}$ represents the toroidally axisymmetric modes of the potential. They are removed so that zonal flows and convection cells are not taken into account. The autocorrelation length L_{AC} of $\delta\phi$ is the Half Width at Half Maximum (HWHM) of the autocorrelation function computed as a function of r, θ and time on a sliding radial window $[r-\delta r_{max}, r+\delta r_{max}]$. A maximum radial extent of $\delta r_{max} = 20\rho_{c,0}$ is sufficient to capture most of the turbulent radial structures. L_{AC} (Figure 4) remains close to $3.5\rho_{c,i}$ with a small $E\times B$ shear rate level $\omega_{E\times B} < 1$ without the source but decreases where the flow shear rate is maximum ($r/a = 0.75$) with

the source turned on. The radial extension of the turbulent structures is effectively reduced locally by the $E \times B$ shear flow. However the correlation length increases in the range $r/a \in [0.2; 0.4]$ and decreases near $r/a = 0.5$ where shearing is not strong ($|\omega_{E\times B}| < 1$). Hence, we cannot attribute the decrease of χ_T and turbulence in those regions to the auto-correlation length reduction.

In the source region, the smallest poloidal scales ($k_\theta \rho_{c,i} > 0.1$) of the poloidal wavenumber spectra of the perturbed potential go through a much more important intensity reduction than the bigger scales ($k_\theta \rho_{c,i} < 0.1$). Since the mean scale is shifting from $\overline{k_\theta \rho_{c,i}} \approx 0.28$ to $\overline{k_\theta \rho_{c,i}} \approx 0.16$, we conclude that turbulent structures undergo a reorganisation due to sheared poloidal flows induced by the vorticity source. Those structures may get *tilted* along the poloidal direction due to the high shearing levels, hence the change in the mean poloidal scale of the turbulent structures.

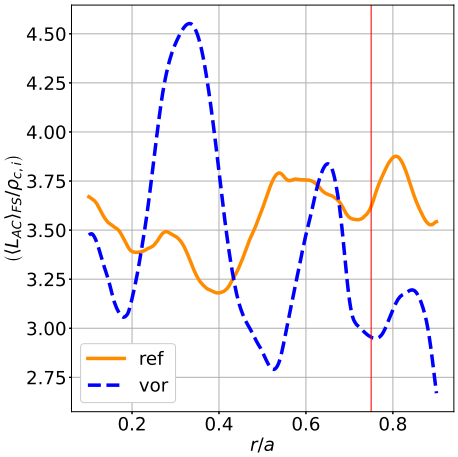

Figure 4: *Flux surface and time average of the correlation length L_{AC} normalized to the local ion gyro-radius as a function of radius* ***without*** *(orange solid line) and* ***with*** *(blue dashed line) the source turned on. The red vertical line indicates the source location for the vorticity case.*

Conclusion

Injecting a strong $E \times B$ shear flow is effective in reducing turbulence intensity and the radial extension of turbulent structures. 5D gyrokinetic simulations show a slight increase in core pressure and a « plateau » forming near the source region, which indicate the presence of a transport barrier mechanism. The total heat flux and turbulent heat diffusivity are significantly diminished in the source region but also slightly reduced in the core region when edge poloidal shearing is in place.

References

[1] Paulett C. Liewer, Nucl. Fusion, vol. 25, no. 5, p. 543, 1985.

[2] F. Wagner et al., Phys. Rev. Lett., vol. 49, no. 19, p. 1408, 1989.

[3] H. Biglari et al., Phys. Fluids B, vol. 2, no. 1, p. 1-4, 1990.

[4] V. Grandgirard et al., Comput. Phys. Commun., vol. 207, pp. 35–68, 2016.

[5] P. Guzdar et al., Phys. Fluids, vol. 26, no. 3, p. 673-677, 1983.

[6] A. Strugarek et al., Plasma Phys. Control. Fusion, vol. 55, no. 7, p. 074013, 2013.

[7] G. Lo-Cascio et al., Nucl. Fusion, 2022 (submitted)